AJR FOCUS ON:

Metal-Induced Artifacts in MRI

Brian A. Hargreaves[1]
Pauline W. Worters[1]
Kim Butts Pauly[1]
John M. Pauly[2]
Kevin M. Koch[3]
Garry E. Gold[1]

OBJECTIVE. The purpose of this article is to review some of the basic principles of imaging and how metal-induced susceptibility artifacts originate in MR images. We will describe common ways to reduce or modify artifacts using readily available imaging techniques, and we will discuss some advanced methods to correct readout-direction and slice-direction artifacts.

CONCLUSION. The presence of metallic implants in MRI can cause substantial image artifacts, including signal loss, failure of fat suppression, geometric distortion, and bright pile-up artifacts. These cause large resonant frequency changes and failure of many MRI mechanisms. Careful parameter and pulse sequence selections can avoid or reduce artifacts, although more advanced imaging methods offer further imaging improvements.

Keywords: distortion, implant, joint replacement, metal artifacts, prosthesis, susceptibility

DOI:10.2214/AJR.11.7364

Received June 14, 2011; accepted without revision June 17, 2011.

Supported by grant R21-008190 from the National Institutes of Health.

[1]Department of Radiology, Lucas Center for Imaging, Rm P270, 1201 Welch Rd, Stanford, CA 94305-5488. Address correspondence to B. A. Hargreaves (bah@stanford.edu).

[2]Department of Electrical Engineering, Stanford University, Stanford, CA.

[3]Applied Science Laboratory, GE Healthcare, Waukesha, WI.

AJR 2011; 197:547–555

0361–803X/11/1973–547

MRI is widely used for clinical evaluation in neurology, oncology, cardiology, and orthopedics to name a few. However, the presence of implanted metallic objects may either render MRI unsafe or greatly limit its diagnostic utility. This presents a tremendous clinical challenge because many of the subjects with implanted devices are precisely the population who may require imaging evaluation. For example, more than 300,000 spinal fusions were performed in 2007 [1], with complications in as many as 30–40% of subjects [2–4]. In 2005, there were 80,000 revision surgeries for total knee and total hip replacements [5]. Metallic implants are also used in surgical reconstruction procedures in which patients may require follow-up imaging. In addition, there are many other smaller devices, such as surgical clips, dental fillings, fixation screws, or surgical pins that alone can complicate imaging techniques.

Many implanted devices are unsafe for MRI. First, ferromagnetic objects can experience strong forces that originate from the static magnetic field [6]. The forces are strongest in regions near the magnet where the field strength changes rapidly over a small distance. Unfortunately, over a small distance (tens of centimeters), forces can change from negligible to strong enough to project an object. Second, some implants can cause heating because of interaction with radiofrequency fields. The most common example is guidewires [7, 8]. Although extensive research has characterized device safety and in some cases improved the ability to detect unsafe devices, no current methods exist to alter the MRI safety of ferromagnetic objects that may experience significant forces or implants that may cause heating.

Although numerous metals are deemed MRI safe, they can still significantly impede imaging for several reasons. First, fundamentally, there is no MRI signal from the metal, so the metal is dark on MR images. This is in contrast to radiographic images in which radiopaque metal is bright. Second, the presence of metal can result in severe variations in the static magnetic field because of susceptibility variations between metal and surrounding tissue [9]. These field variations depend on the size, shape, and type of metal as well as orientation in the magnetic field.

The magnetic field variations cause large resonant frequency variations, resulting in a variety of artifacts in MRI. When the field changes rapidly with position, there is significant dephasing of the signal, resulting in signal loss. This static effect can be avoided by using spin-echo sequences or sometimes by using very short echo-time gradient-echo sequences. The frequency variations can also prevent successful use of fat-suppression techniques that are based on the chemical shift, or frequency difference between fat and water tissues. In both the slice selection

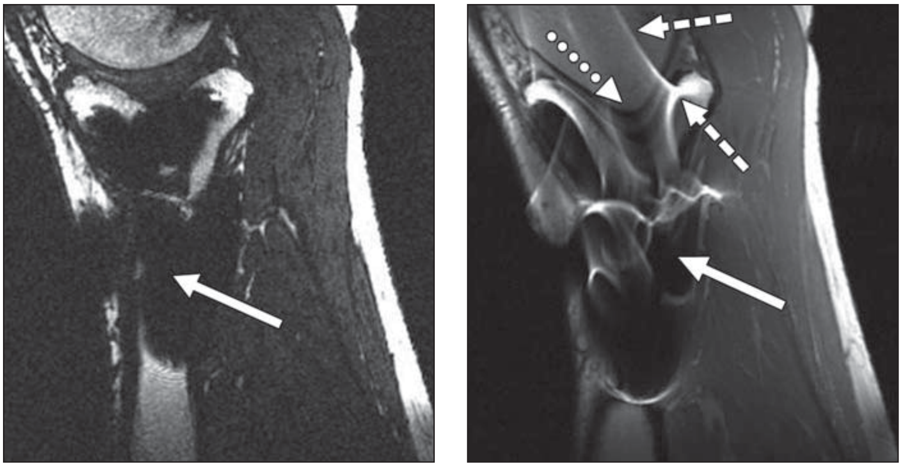

Fig. 1—Examples of artifacts due to presence of stainless steel screws in healthy 37-year-old man.
A and **B,** In gradient-echo image with ± 62.5 kHz receive bandwidth (**A**) and spin-echo image with ± 16 kHz receive bandwidth (**B**), solid arrows show signal loss that can be due to dephasing or from signal being shifted away from region. Dotted arrow in **B** shows geometric distortion of femoral condyle, and dashed arrows show signal pile-up, which can be combination of in-plane and through-slice displacement of signal from multiple locations to one location.

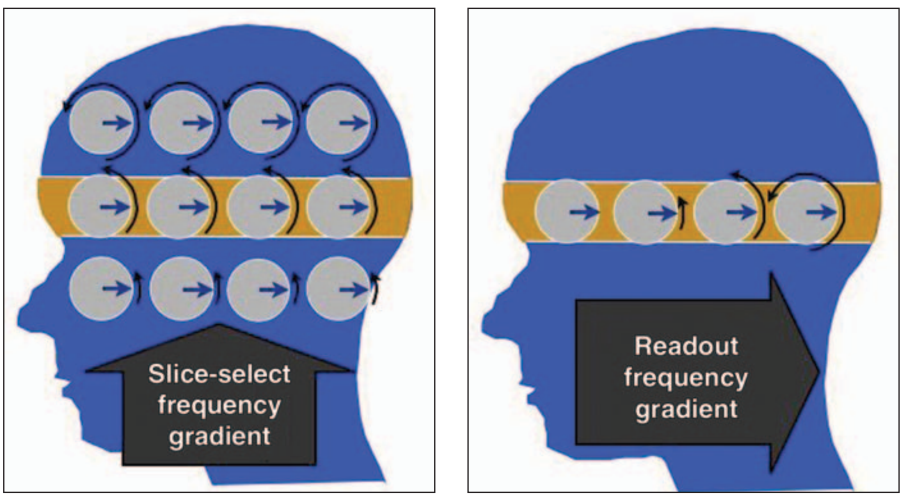

Fig. 2—Magnetization dynamics for selective excitation and imaging readout.
A and **B**, Drawings show magnetization dynamics during slice selection (**A**) and imaging readout (**B**). Magnetization precession rate or frequency is indicated by black arrows showing different amounts of phase (rotation). To excite orange slice (**A**), gradient is turned on in slice-select direction (superior-inferior) to impose frequency variation. Radiofrequency pulse is played at frequency of desired slice. Once slice has been excited (**B**), slice-select gradient is turned off, and gradient is turned on in readout or frequency-encode direction (anterior-posterior). This imposes frequency variation with position. Received signal then consists of multiple frequencies, strength of which depends on amount of signal at corresponding position.

and readout directions, frequency variations result in displacement of signal. Because the frequency varies spatially, signal can be shifted away from regions, resulting in signal loss, or can accumulate in one region, resulting in a pile-up artifact. In less-extreme situations, the varying displacements result in geometric distortion of the image. Several of these artifacts are illustrated in Figure 1.

In this article, we review some of the basic principles of imaging, and how metal-induced susceptibility artifacts originate in images. We describe common ways to reduce or modify artifacts using readily available imaging techniques. Next we describe advanced methods to correct readout-direction artifacts and slice-direction artifacts. Although technical, this article focuses on practical methods and techniques of artifact reduction. More advanced methods as well as thorough physical explanations of the origin of susceptibility artifacts have been recently described [10].

Imaging Mechanisms

We will briefly review the physics of MRI to explain why the presence of metal causes artifacts in imaging. MRI is enabled by first polarizing nuclear spins, typically in a static magnetic field. At macroscopic levels, the nuclear spins are collectively referred to as magnetization, which is a vector quantity. The magnetization can be excited or actively rotated away from the direction of the static magnetic field to point in a transverse direction by a radiofrequency magnetic field. The transverse magnetization then precesses or resonates around the direction of the static field, which can generate a radiofrequency signal in a receive coil. The use of gradient fields can change the precession rate as a function of position in an arbitrary direction, allowing image formation in arbitrary scanning orientations.

Most MRI methods consist of exciting the magnetization in slices and forming 2D images of each slice. Excitation is achieved by first using a slice-select gradient that imposes a variation of precession rate (or resonance frequency) in the slice direction (Fig. 2A). Next, a radiofrequency magnetic field is generated, with a limited bandwidth around a center frequency that is chosen so as to excite magnetization at a particular position. This is analogous to setting the dial on an amplitude-modulation (AM) radio to tune to a particular radio station. In MRI, after the spins within the slice have been excited, the excitation gradient is turned off and the variation of precession rate in the slice direction is removed.

To form 2D images, a gradient field can be turned on in a direction within the plane of the slice, causing a variation of the precession rate

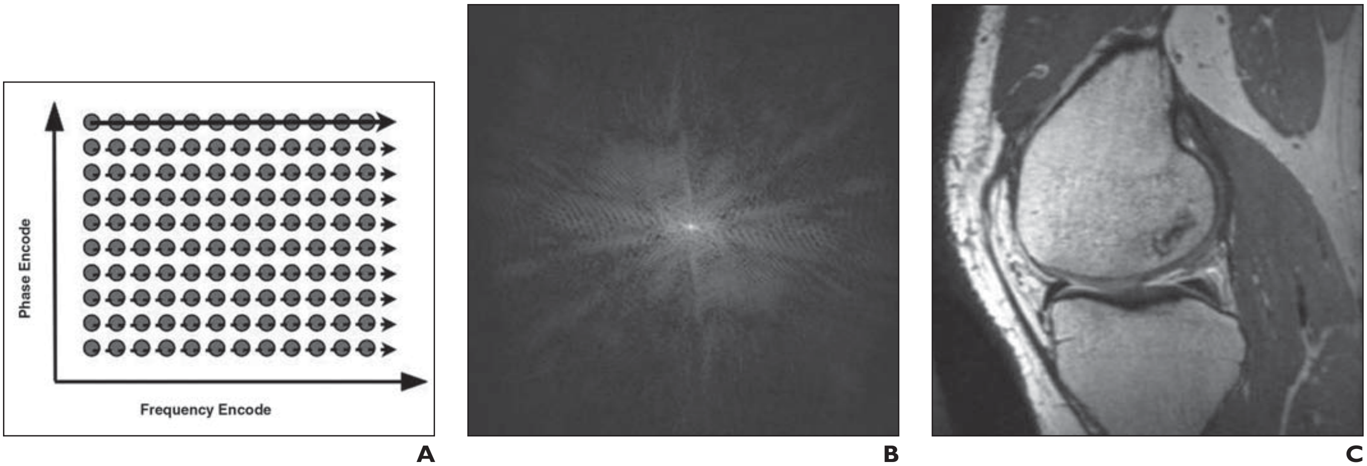

Fig. 3—Samples in k-space.
A, In conventional MRI, samples of data are acquired in k-space. On each excitation, samples are taken along a line of locations in frequency-encode direction over time (*solid* and *dashed arrows*). On different excitations, location of these samples in phase-encode direction is changed.
B and **C,** Sampled data in k-space (**B**) consists of signal strengths at each location and can be Fourier transformed to obtain corresponding image (**C**).

(Fig. 2B). The received signal is acquired during this time. The individual frequencies (or tones) can be assigned to specific image locations using a method called a Fourier transform, with the amplitude of each frequency corresponding to the strength of the magnetization at a particular position. This process, called frequency encoding, is analogous to hearing a piano sound: If several keys are pressed on a piano with different strength, the strings cause a vibration in your ear, analogous to the MRI signal that is recorded. Your ear is able to deduce the individual tones as well as the strength of each, much like the Fourier transform process deduces signal from different locations.

During frequency encoding, the received signal is actually sampled at discrete time points, with the change between points due only to the position of the sample points and the area of the gradient waveform between them. Unlike frequency encoding, phase encoding switches on a gradient for a finite time, then switches it off before acquiring samples. On successive excitations, the amplitude of the gradient can be changed. This allows sampling of the 2D data space, k-space, as shown in Figure 3. The Fourier transform can be applied in two directions, leading to a 2D image. A key distinction between phase encoding and frequency encoding is that the excitation-to-acquisition time for a data sample depends only on its position in the readout direction.

Although the raster scanning of k-space using frequency and phase encoding (Fig. 3) is by far the most common method of acquiring MR images, other options exist. Just as phase encoding moves to a different sample position in k-space, any combination of gradients can be used to move to any position. Sampling several lines of k-space on one excitation using echo-planar imaging is a common option [11]. Alternatively, sampling with a radial [12] or spiral [13] pattern is also used for certain applications. These "non-Cartesian" sampling methods have advantages and disadvantages compared with raster scanning, and the artifacts due to the presence of metal may differ substantially from those discussed here for Cartesian scanning methods.

Image Artifacts Near Metal Implants

The most prominent image artifacts that occur with imaging near metal arise from the inhomogeneous static magnetic field, which causes large variations in the precession rate (or resonant frequency) across the object. The predominant artifacts that arise in imaging are signal loss due to dephasing, failure of fat suppression, and displacement artifacts. Displacement artifacts occur in the slice selection and readout directions and include geometric distortion, signal loss, and signal pile-up.

Near metal objects, the magnetic field variations can be very rapid, such that the magnetization within a single imaged voxel precesses at varying rates. This leads to dephasing or loss of coherence and signal loss. In images, this manifests as a black area in which there would otherwise be signal (Fig. 1). Fortunately, dephasing effects can be almost completely avoided by the use of spin-echo imaging, as described later.

Aside from the distortion and dephasing artifacts described, an important detrimental effect of imaging near metal is failure of fat suppression. Many fat-suppression techniques are far more sensitive to magnetic field variations than the image-formation methods themselves. The most common method of fat suppression is to use chemically selective saturation, often called fat saturation [14]. This method selectively excites fat, exploiting the fact that the fat resonance is 220 Hz below that of water at 1.5 T. The frequency shifts near metallic implants can range from about 3 to 80 kHz. This can cause large changes in the fat resonance, easily enough to cause complete failure of fat saturation because the saturation pulse completely misses the resonant frequency of fat near metal.

As described, the method of selectively exciting a 2D slice in MRI is to apply a radiofrequency magnetic field of finite bandwidth in the presence of a gradient field. Because the gradient maps position to resonant frequency, the slice position is determined by changing the frequency of the radiofrequency field. Variations in the static magnetic field cause an error in the position that is selected. The error can cause a shift in the excited slice, or a curving or "potato-chip" effect. It can also cause the slice to be thicker or thinner than desired and can even result in splitting of the slice into multiple regions. The overall result is that the selected region differs from what was desired, and therefore, the desired slice position no longer represents the location of the image. Although small shifts or curving of the slice may not be noticeable, the thinning and thickening lead to clear signal loss or pile-up effects, the

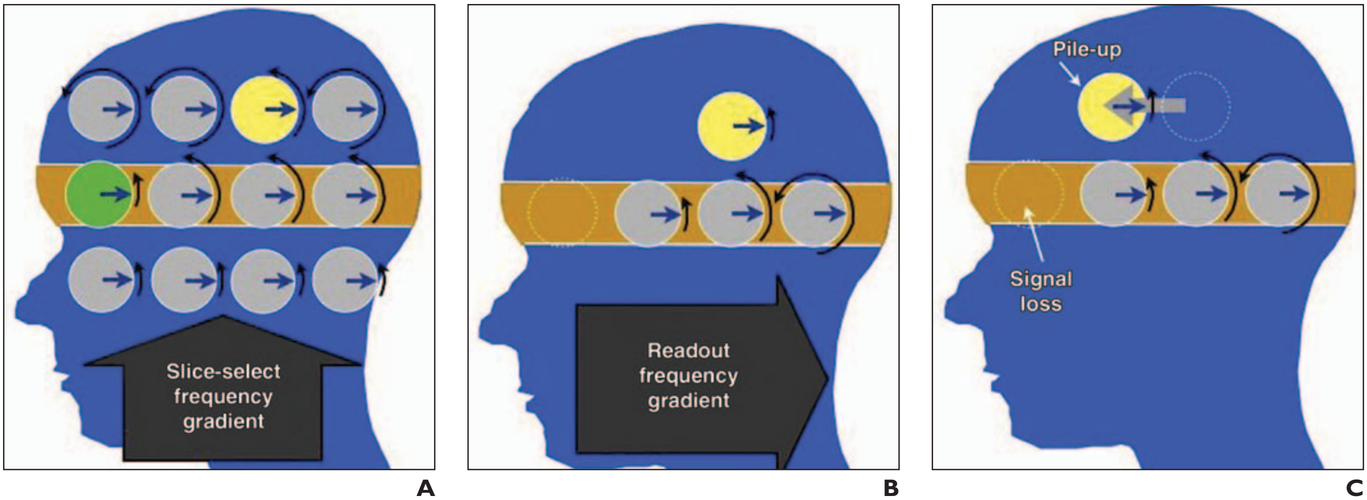

Fig. 4—Magnetization dynamics with off-resonsance.
A–C, Effect of offset of resonance frequency or off-resonance on slice selection (**A**) and imaging readout (**B**). During slice selection, yellow and green spins resonate below expected rates. When radiofrequency pulse is centered at rate of gray spins in orange region, green spin is not excited, while yellow spin is excited, resulting in signal loss (green) and pile-up (yellow). Next, when spins are imaged, yellow spin will again resonate below expected rate (**B**) and be detected at incorrect position in anteroposterior direction (**C**), resulting in in-plane pile-up artifact. Note that although only a few spins are shown here to illustrate concept, there is actually continuous distribution of magnetization in both directions, and excited slice can show displacement, broadening, thinning, or even splitting depending on off-resonance frequency distribution.

mechanisms of which are shown in Figure 4. Using the radio-tuning analogy, the presence of the metal effectively causes some radio stations to transmit at the wrong frequency, so that when you tune to a location you may miss the station you are seeking, hear the wrong station, or hear multiple stations that are transmitting on the same channel.

During image acquisition in the frequency-encoding direction, a gradient field is generated to map the position to particular precession rates of the magnetization. The reconstruction inverts this process by identifying the tones in the signal, with each tone corresponding to a position. However, variations in the static magnetic field cause shifts in these tones, which again result in an error in determining the position from which the signal originates. Like slice distortion, the variations can result in bulk shifts that can distort the image or, in more extreme cases, signal loss or pile-up effects when the signal is shifted away from a position or when signal from multiple positions is shifted to one position. The mechanisms of slice-select and frequency-encode distortion are shown in Figure 4. Note that the frequency-encode-direction and slice-direction artifacts are difficult to separate because both result in geometric distortion, signal loss, and signal pile-up effects. Using the piano analogy, the static field variations simply cause the piano to be grossly out of tune and generate the wrong sounds for certain keys. A listener trying to identify the tones will make errors that correspond to shifts of signal to and from different positions in the image. In extreme cases, one key may generate the tone of the adjacent key, resulting in the perception of increased signal at that tone (pile-up) or loss at the missing tone.

Basic Reduction of Artifacts

Although artifacts near metal can be severe, it is important to realize that many standard techniques and careful parameter selections can be combined to mitigate them, often to the point that an image has diagnostic value in spite of artifacts. The main types of artifacts and both basic and advanced methods to reduce them are summarized in Table 1.

The signal dephasing that occurs when the static magnetic field varies rapidly results in dark areas of signal loss. The most common way to avoid this is to use spin-echo techniques, which use a 180° refocusing pulse that reverses static field dephasing. As shown in Figure 1, the spin-echo avoids much of the signal loss seen with gradient-echo imaging. An alternative to using spin-echoes is to use ultrashort TE methods in which imaging is performed immediately after the radiofrequency

TABLE 1: Common Artifacts in MRI Due to Presence of Metallic Implants and Methods to Reduce Them

Artifact	Standard Methods to Reduce Artifact	Advanced Methods to Reduce Artifact
Signal loss from dephasing	Spin-echo or FSE (FSE, TSE, RARE)	Ultrashort echo-time sequences, SWIFT
Failure of fat suppression	Use of STIR imaging or Dixon techniques (less effective)	
Geometric distortion	High-readout bandwidth	View-angle tilting, field map–based corrections
In-plane distortion (pile-up and signal loss)	High-readout bandwidth, swap frequency or phase	View-angle tilting
Through-slice distortion	Nonselective Imaging, thin slices	Multispectral imaging (MAVRIC, SEMAC, etc.)
All distortions	All listed combinations	Multispectral imaging (MAVRIC, SEMAC, etc.)

Note—Standard methods are widely available, whereas more advanced methods are generally in research phases. FSE = fast spin-echo, TSE = turbo spin-echo, RARE = rapid acquisition with relaxation enhancement, SWIFT = sweep imaging with Fourier transform, MAVRIC = multiacquisition variable-resonance image combination, SEMAC = slice-encoding for metal artifact correction.

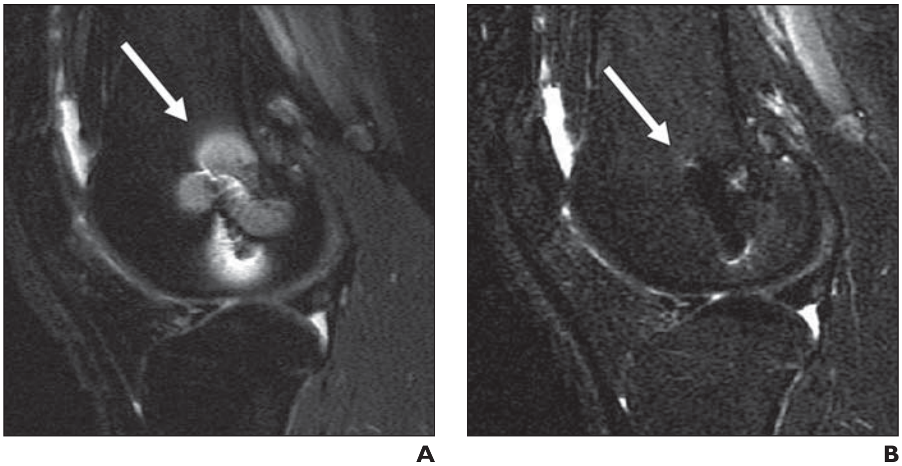

Fig. 5—Patient with titanium screw in knee.
A and **B,** Conventional fat-saturated (**A**) and STIR (**B**) proton density–weighted images of knee show fat-saturation leads to imperfect fat suppression near metal (*arrow*), but maintains signal-to-noise ratio (SNR), whereas STIR provides uniform fat suppression but decreases SNR and still shows some pile-up artifacts around metal.

excitation so that there is less time for magnetization to become incoherent (or dephase).

The failure of fat suppression can be reduced in many cases by the choice of fat suppression technique. Common MRI fat-suppression methods include spectrally-selective saturation [14], STIR [15], or multiple-echo separation techniques such as Dixon separation [16, 17]. Fat-suppression or water-only excitations are the most sensitive to the presence of metal, and will fail any time the shim is insufficient to remove background frequency variations to within the chemical shift frequency difference between fat and water. Dixon techniques can track gradual magnetic field variations and perform well some distance from metal where fat saturation may fail. However, closer to the metal, even Dixon techniques fail, and the best choice is to use STIR imaging because it is completely independent of resonance frequency. STIR uses an inversion recovery approach to null fat on the basis of its short T1 relaxation time, which provides much more homogeneous fat suppression near metal, as shown in Figure 5. There are two downsides of using STIR. First it is limited by the low signal-to-noise ratio (SNR) because the inversion pulse causes attenuation of the nonfat signal. Second, when a contrast agent is used, the tissue that normally enhances would instead be suppressed because of the shortened T1. Therefore, for contrast-enhanced imaging in the presence of metal, the options are limited. Dixon-based methods are probably the best option but will certainly fail near larger implants.

The spatial distortion in the slice direction (Fig. 4) is the ratio of frequency offset to slice bandwidth, multiplied by slice width. Therefore, using thin slices will reduce the amount of this distortion. The cost of this is both increased scanning time because more slices are required to adequately cover the volume of interest and reduced SNR because the voxel size has been reduced. Multiple slices can be averaged during postprocessing to recover some SNR, but this technique still reduces the overall SNR efficiency by the square-root of the number of slices averaged. Nonetheless, the use of thin slices is a viable distortion-reducing option that can by used on most scanners.

A direct way to reduce distortion effects is to maximize the bandwidth used both during slice selection and during readout. On both

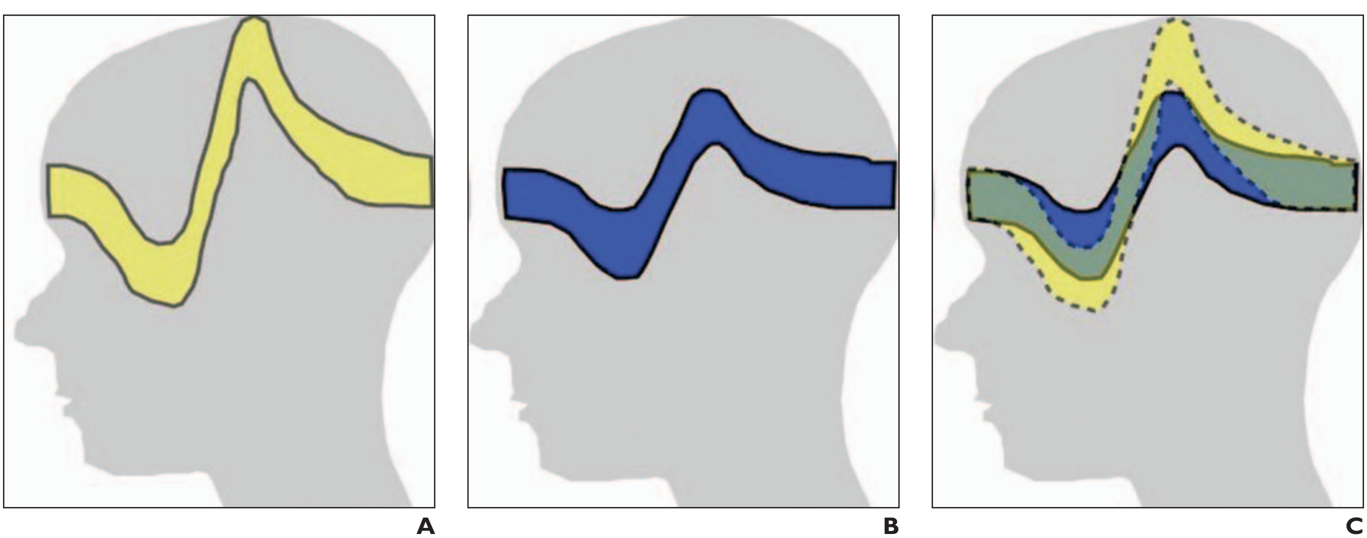

Fig. 6—Effect of slice-selection bandwidth on slice.
A, Drawing shows use of low slice-selection bandwidth results in substantial slice distortion, or "potato-chipping," in presence of frequency variations.
B, Drawing shows use of higher excitation pulse bandwidth decreases distortion, but at cost of higher radiofrequency power.
C, Drawing shows use of unmatched bandwidths on excitation and refocusing pulses so that only overlapped region is imaged. This may reduce some artifacts but can also result in signal loss.

slice selection and readout, the spatial distortion is inversely proportional to the gradient strength, which scales with the bandwidth. Some systems will allow the use of increased bandwidth radiofrequency slice-selection pulses, which will thus reduce slice distortion, as shown in Figure 6. Increased radiofrequency bandwidth, however, comes at a cost of increased power deposition (specific absorption rate [SAR]), which may either force longer TRs or fewer interleaved slices per repetition.

As with slice selection, maximizing the readout bandwidth will minimize displacement artifact in the readout direction. The number of pixels of in-plane displacement is simply the ratio of the frequency offset to the bandwidth per pixel. Note that on many systems, the readout bandwidth is specified using the half bandwidth over the FOV. The pixel bandwidth is twice the half bandwidth divided by the readout matrix size. As with the slice-selection bandwidth, increasing the readout bandwidth comes at a cost—SNR. Maximizing readout bandwidth reduces echo spacing, which leaves an option for longer echo trains to partly compensate for lost efficiency. Next to using spin-echo methods, maximizing readout bandwidth is probably the simplest way to dramatically reduce artifacts near metal.

Most conventional imaging sequences will suffer from displacement artifacts in both the slice-select direction and the readout direction but not in the phase-encode direction. In 3D sequences, although there are two phase-encode directions, there is typically a slab-selective excitation that has very large distortions because, again, the distortion is proportional to the slice (or slab) thickness. However, if a nonselective pulse is used with 3D sequences, there will indeed be two phase-encode directions, neither subject to displacement artifacts. In certain imaging scenarios, the phase-encode direction can be positioned in the direction perpendicular to interfaces so that the interfaces can still be clearly seen in spite of artifacts [18, 19].

Recall that the displacement due to off-resonance effects during excitation is inversely proportional to the radiofrequency bandwidth. In general, where spin-echo sequences are used, an option is to use a different radiofrequency bandwidth for the excitation and refocusing pulses. This causes a different displacement for the excited and refocused slices in the presence of frequency offsets (Fig. 6). The result is that no signal arises from the off-resonant tissue because it is not refocused. This approach is similar to inner-volume imaging, in which the region is limited by changing the spatial region that is excited and refocused. The use of differing bandwidths has the trade-off that artifacts may be suppressed but at a cost that some signal is lost. In addition, the different excitation and refocusing regions can result in increased saturation of adjacent slices, which may force increased scanning times, larger slice gaps, or other compromises. Differing excitation and refocusing pulse bandwidths are already used in cases to reduce artifacts from gradient nonlinearity and may be used where the refocusing pulse bandwidth is reduced because of peak radiofrequency limits. However, more recently, this concept has been used specifically to reduce artifacts near metal implants [20].

In-Plane Artifact Reduction

The in-plane artifacts because of displacement include geometric distortion and, in more severe cases, signal loss and pile-up artifacts. Although maximizing bandwidth is helpful in all cases, there are other options that can improve quality further.

The displacements due to off-resonance are predictable when the frequency error is known. In cases of fairly smooth frequency error, the geometric distortion can be largely fixed. The key assumption to this approach is that the frequency changes can be resolved by the image resolution or, put another way, that one frequency offset is representative for each voxel. The process then consists of measuring this frequency offset using field-mapping techniques, typically with multiple TEs. The image can then be distorted in the reconstruction to correct the geometric distortions that result from frequency offsets.

Field mapping is unable to resolve the very rapid spatially varying frequency offsets that lead to pile-up and signal loss. A method called view-angle tilting can be quite powerful in this situation [21]. View-angle tilting takes advantage of the fact that the slice displacement and in-plane displacement because of off-resonance have a constant ratio. View-angle tilting replays the slice-selection gradient during the readout, which shears the image in the plane of the slice and readout directions. The result is that slice displacements exactly cancel in-plane displacements, so the in-plane displacements are removed as shown in Figure 7. However, view-angle tilting does not fix the slice distortion. Note that an alternative view of view-angle tilting is that the radiofrequency pulse excites a certain bandwidth. By replaying the slice select gradient, the off-resonance is limited to the radiofrequency bandwidth, and in-plane distortion is nearly removed [22]. A limitation of view-angle tilting, however, is that the readout duration is limited to that of the radiofrequency excitation; otherwise, blurring can result [23]. This limits the SNR or spatial resolution that can be achieved. To avoid this blurring and to minimize residual artifact from the voxel tilt,

A

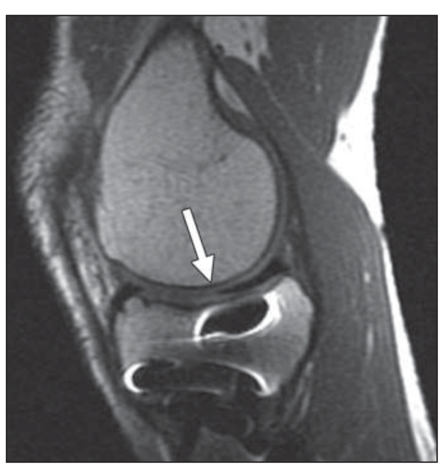

B

Fig. 7—37-year-old man with stainless steel screws in tibia.
A and **B,** Spin-echo (**A**) and view-angle tilting (**B**) images obtained using identical parameters show geometric distortion is completely corrected in view-angle tilting (*arrows*) but through-slice signal loss and pile-up artifacts remain (bright areas in tibia).

a high-bandwidth readout is desirable when using view-angle tilting [24].

One approach that has been used to reduce in-plane artifacts is to limit the excited bandwidth. This can be achieved using a spectral-spatial excitation, which excites both a limited slice and a limited band of frequencies. The frequency range is limited, thus limiting the in-plane artifact. The cost of this approach is that the excitation must be repeated for different frequencies, which costs scanning time.

Through-Plane Artifact Reduction

Slice-direction distortion is a challenge because maximizing radiofrequency bandwidths is ultimately limited by the maximum radiofrequency amplitude as well as the radiofrequency power or SAR. Methods have been designed to correct linear field variations in the slice direction. Gradient-echo slice excitation profile imaging uses slice-direction phase-encoding and a Fourier transform to recover signal losses in each slice [25], and 3D *z*-shimming builds on this with more efficient sampling on the basis of expected field variations [26]. An alternative approach is to acquire and use a field-map to estimate the slice displacement and thickening or thinning, which can be corrected in some cases [27]. More recently, methods have built on these techniques to correct a much more arbitrary range of resonance frequency offsets near metal.

Multiacquisition variable-resonance image combination (MAVRIC) is a method to correct both in-plane and through-slice displacement artifacts [28]. MAVRIC uses a frequency-selective excitation (rather than exciting a slice or slab) to limit the range of frequency offsets imaged at one time. This is followed by a standard 3D imaging readout, typically using a spin-echo train. As described earlier, when the range of frequencies is limited, the in-plane displacement is also limited, to within about a pixel in this case. MAVRIC avoids slice-direction displacement by using phase encoding to resolve in this direction. The 3D images are repeated for a range of frequencies and combined together, typically using a sum-of-squares operation. The combined images have minimal artifact and include signal from a wide range of frequency offsets near metal.

Slice-encoding for metal artifact correction (SEMAC) also corrects both in-plane and through-slice distortions near metal [29]. In SEMAC, 2D slices are excited just as in a standard multislice sequence, resulting in distorted profiles. For each slice, a 3D image is formed, using view-angle tilting to avoid in-plane artifacts and phase-encoding in the other two directions to avoid distortion. By combining the 3D images for each slice, a distortion-corrected volume can be achieved.

MAVRIC and SEMAC are similar in many respects. Both use multiple excitations to excite the overall volume being imaged, and both use a 3D spin-echo acquisition to resolve through-plane distortion. In both cases, the residual distortion in the readout direction is identical, within about a pixel. The fundamental difference between the techniques is that MAVRIC excites limited frequency bands, whereas SEMAC excites limited spatial bands. However, note again that the spatial bands are distorted by frequency offsets. There are other implementation differences, including whether the excitation bands overlap, but these can typically be applied equally to both methods. A hybrid MAVRIC-SEMAC approach merges features from both original methods into one sequence [30]. Figure 8 shows how individual regions are excited in MAVRIC, SEMAC, and the hybrid technique, whereas Figure 9 shows example images using all of these methods.

Other methods have also recently been proposed for imaging near metal. Ultrashort TE methods and swept imaging with Fourier transform are alternatives to spin-echo methods for avoiding static dephasing [31, 32]. Both methods typically use a radial acquisition, which results in blurring, but near metal there are more extreme additional displacement and

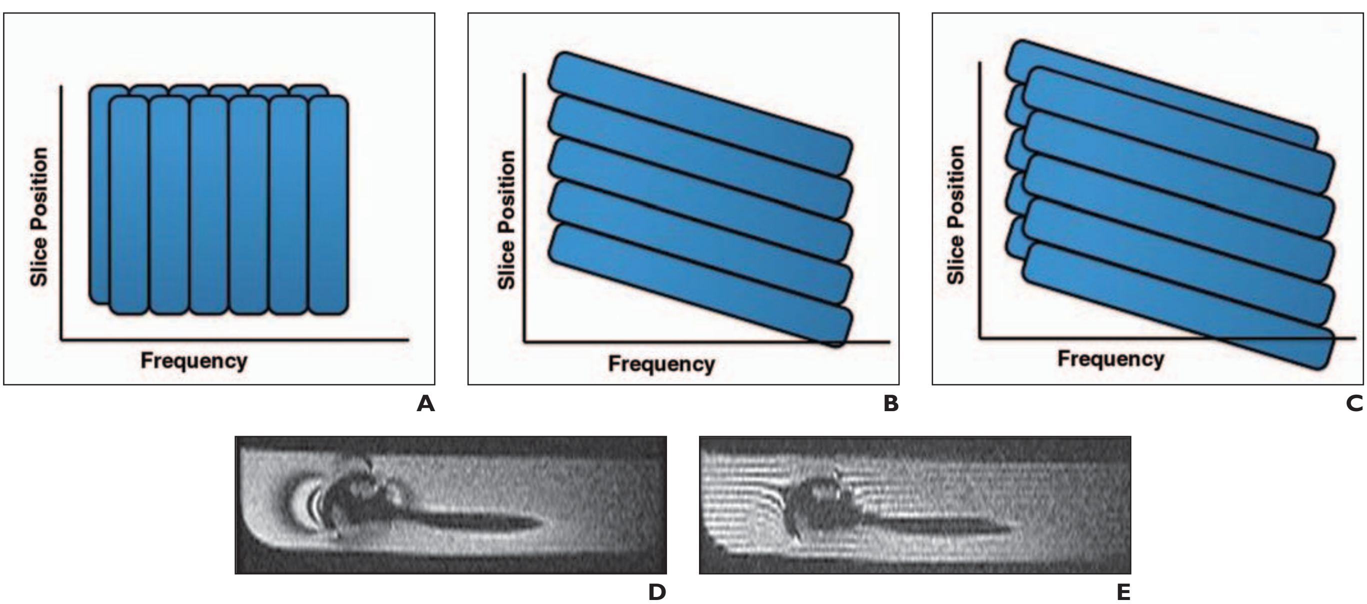

Fig. 8—Multiacquisition variable-resonance image combination (MAVRIC) and slice-encoding for metal artifact correction (SEMAC).
A and **B,** Excited regions of MAVRIC (**A**) and SEMAC (**B**) differ in that MAVRIC is purely frequency selective, whereas SEMAC is spatially selective but with spatial shifts due to frequency. Original MAVRIC method proposes overlapped regions, which improves artifact suppression at cost of time.
C, Hybrid approach uses spatially-selective excitation but overlapped regions.
D and **E,** In phantom with shoulder prosthesis, regions can be illustrated by intentionally leaving space between regions and showing reformatted images. In MAVRIC (**D**), regions follow contours of magnetic field variations, whereas in SEMAC (**E**) regions are distorted ("potato-chipped") slices.

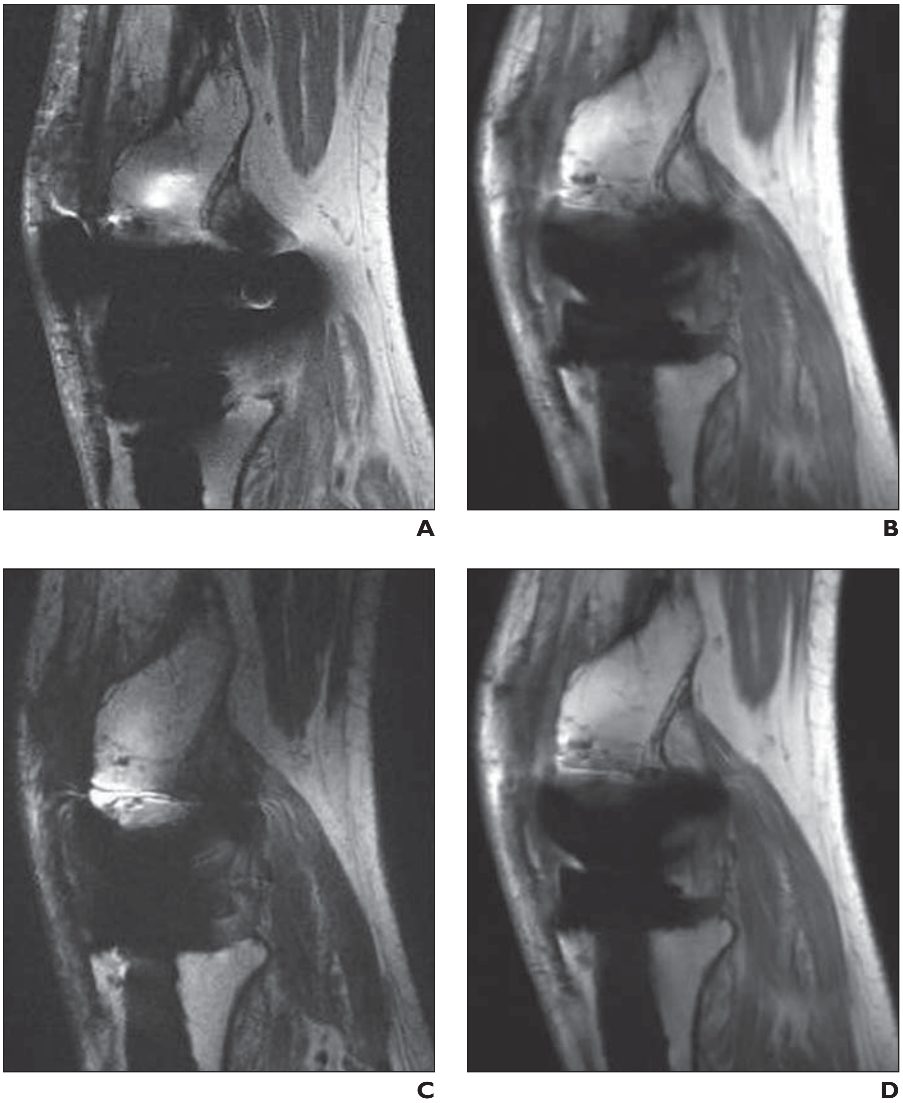

Fig. 9—Different approaches in patient with total knee arthroplasty.
A–D, Example images using spin-echo (**A**), multiacquisition variable-resonance image combination (MAVRIC) (**B**), slice-encoding for metal artifact correction (SEMAC) (**C**), and MAVRIC-SEMAC (**D**). Signal loss and pile-up artifacts in spin-echo image are substantially reduced with three correction techniques, with similar overall ability to depict tissue near implant.

pile-up artifacts. As with other methods, for a high-readout bandwidth these artifacts can be reduced [33] but have not been compared directly with MAVRIC or SEMAC. Furthermore, the very short TEs may allow visualization of the polyethylene spacer, which could have diagnostic value [34]. The non-Cartesian methods add additional implementation complexity, which also has limited their use for routine scanning.

Summary

Although some metallic implants are safe for MRI, their presence can cause substantial artifacts in images, including signal loss, failure of fat suppression, geometric distortion, and signal pile-up. Signal loss caused by static dephasing can largely be corrected by the use of spin-echoes, and some distortion can be reduced by the choice of scanning parameters. Fat-suppression failure is mitigated by using Dixon-based techniques or, better yet, STIR imaging at a cost of SNR. Displacement artifacts that cause geometric distortion, signal loss, and pile-up can be corrected with a variety of methods. View-angle tilting is effective for in-plane displacement artifacts. However, much more complete correction, including correction for both in-plane and through-slice displacements, can be achieved by multispectral imaging methods such as MAVRIC or SEMAC but at a cost of increased scanning time. All of these methods are now or soon will be fairly readily available on most scanners. Overall, it is important to understand the cause of metal-induced artifacts and to select the most appropriate of the available options to reduce or avoid artifacts in the particular application.

References

1. Elixhauser A, Andrews RM. Profile of inpatient operating room procedures in US hospitals in 2007. *Arch Surg* 2010; 145:1201–1208
2. Javid M, Hadar E. Long-term follow-up review of patients who underwent laminectomy for lumbar stenosis: a prospective study. *J Neurosurg* 1998; 89:1–7
3. Mekhail N, Wentzel D, Freeman R, Quadri H. Counting the costs: case management implications of spinal cord stimulation treatment for failed back surgery syndrome. *Prof Case Manag* 2011; 16:27–36
4. Ryken T, Eichholz K, Gerszten P, Welch W, Gokaslan Z, Resnick D. Evidence-based review of the surgical management of vertebral column metastatic disease. *Neurosurg Focus* 2003; 15:E11
5. Kurtz S, Ong K, Lau E, Mowat F, Halpern M. Projections of primary and revision hip and knee arthroplasty in the United States from 2005 to 2030. *J Bone Joint Surg Am* 2007; 89:780–785
6. Kanal E, Shellock F, Talagala L. Safety considerations in MR imaging. *Radiology* 1990; 176:593–606
7. Wildermuth S, Dumoulin C, Pfammatter T, Maier S, Hofmann E, Debatin J. MR-guided percutaneous angioplasty: assessment of tracking safety, catheter handling and functionality. *Cardiovasc Intervent Radiol* 1998; 21:404–410
8. Nitz WR, Oppelt A, Renz W, Manke C, Lenhart M, Link J. On the heating of linear conductive structures as guide wires and catheters in interventional MRI. *J Magn Reson Imaging* 2001; 13:105–114
9. Schenck JF. The role of magnetic susceptibility in magnetic resonance imaging: MRI magnetic compatibility of the first and second kinds. *Med Phys* 1996; 23:815–850
10. Koch K, Hargreaves B, Pauly K, Chen W, Gold G, King K. Magnetic resonance imaging near metal implants. *J Magn Reson Imaging* 2010; 32:773–787
11. Mansfield P. Multiplanar image formation using NMR spin-echoes. (letter) *J Phys C Solid State Phys* 1977; 10:L55
12. Lauterbur P, Lai C. Zeugmatography by reconstruction from projections. *Nuclear Science IEEE Trans* 1980; 27:1227–1231
13. Meyer CH, Hu BS, Nishimura DG, Macovski A.

Fast spiral coronary artery imaging. *Magn Reson Med* 1992; 28:202–213
14. Keller PJ, Schmalbrock P. Multisection fat-water imaging with chemical shift selective presaturation. *Radiology* 1987; 164:539–541
15. Bydder GM, Pennock JM, Steiner RE, Khenia S, Payne JA, Young IR. The short TI inversion recovery sequence: an approach to MR imaging of the abdomen. *Magn Reson Imaging* 1985; 3:251–254
16. Dixon WT. Simple proton spectroscopic imaging. *Radiology* 1984; 153:189–194
17. Glover GH. Multipoint Dixon technique for water and fat proton and susceptibility imaging. *J Magn Reson Imaging* 1991; 1:521–530
18. Sofka CM, Potter H, Figgie M, Laskin R. Magnetic resonance imaging of total knee arthroplasty. *Clin Orthop Relat Res* 2003; 406:129–135
19. Potter H, Nestor B, Sofka C, Ho S, Peters L, Salvati E. Magnetic resonance imaging after total hip arthroplasty: evaluation of periprosthetic soft tissue. *J Bone Joint Surg Am* 2004; 86:1947–1954
20. Bos C, den Harder CJ, van Yperen G. MR imaging near orthopedic implants with artifact reduction using view-angle tilting and off-resonance suppression. (abstr) *Proceedings of the International Society for Magnetic Resonance in Medicine18th scientific meeting.* Stockholm, Sweden: International Society for Magnetic Resonance in Medicine, 2010:129
21. Cho Z, Kim D, Kim Y. Total inhomogeneity correction including chemical shifts and susceptibility by view angle tilting. *Med Phys* 1988; 15:7–11
22. Olsen RV, Munk PL, Lee MJ, et al. Metal artifact reduction sequence: early clinical applications. *RadioGraphics* 2000; 20:699–712
23. Butts K, Pauly JM, Gold GE. Reduction of blurring in view angle tilting MRI. *Magn Reson Med* 2005; 53:418–424
24. Kolind SH, MacKay AL, Munk PL, Xiang QS. Quantitative evaluation of metal artifact reduction techniques. *J Magn Reson Imaging* 2004; 20:487–495
25. Yang QX, Williams GD, Demeure RJ, Mosher TJ, Smith MB. Removal of local field gradient artifacts in T2*-weighted images at high fields by gradient-echo slice excitation profile imaging. *Magn Reson Med* 1998; 39:402–409
26. Glover G. 3D *z*-shim method for reduction of susceptibility effects in BOLD fMRI. *Magn Reson Med* 1999; 42:290–299
27. Butts K, Gold GE. Correction of slice profile distortions from metallic devices. (abstr) *Proceedings of the International Society for Magnetic Resonance in Medicine 14th scientific meeting.* Seattle, WA: International Society for Magnetic Resonance in Medicine, 2006:2380
28. Koch KM, Lorbiecki JE, Hinks RS, King KF. A multispectral three-dimensional acquisition technique for imaging near metal implants. *Magn Reson Med* 2009; 61:381–390
29. Lu W, Pauly KB, Gold GE, Pauly JM, Hargreaves BA. SEMAC: slice encoding for metal artifact correction in MRI. *Magn Reson Med* 2009; 62:66–76
30. Koch KM, Brau ACS, Chen W, et al. Imaging near metal with a MAVRIC-SEMAC hybrid. *Magn Reson Med* 2011; 65:71–82
31. Gold GE, Thedens D, Pauly J, et al. MR imaging of articular cartilage of the knee: new methods using ultrashort TEs. *AJR* 1998; 170:1223–1226
32. Idiyatullin D, Corum C, Park JY, Garwood M. Fast and quiet MRI using a swept radiofrequency. *J Magn Reson* 2006; 181:342–349
33. Carl M, Du J, Koch K. Investigations on imaging near metal with combined 3D UTE-MAVRIC. (abstr) *Proceedings of the International Society for Magnetic Resonance in Medicine19th scientific meeting.* Montreal, QC, Canada: International Society for Magnetic Resonance in Medicine, 2011:2668
34. Rahmer J, Bornert P, Dries S. Assessment of anterior cruciate ligament reconstruction using 3D ultrashort echo-time MR imaging. *J Magn Reson Imaging* 2009; 29:443–448